

# Computing 2-D Affine Transform of Boundaries from Points of Significant Curvature

T. Rachidi\* and L. Spacek

Department of Computer Science  
University of Essex  
Colchester CO4 3SQ  
U.K.

## Abstract

*Finding the parameters of the 2-D affine transform is posed as a correspondence problem between points of significant curvature along curves. The algorithm developed for this purpose is simple and intuitive. It uses natural ordering of such points along curves, the uniformity of the expansion factor, and the angle of rotation to constrain the search for the true match. The parameters of the transform – namely the expansion, translation and rotation – are then evaluated from the positions of matched points of significant curvature rather than from curvature values as done by other techniques. This novel technique is robust and copes particularly well with occlusion problems at curve ends. We also show that this technique can be applied to the problem of determining the axes of symmetry.*

## 1 Introduction

An important task in computer vision and image processing is to determine the transformation which maps a 2-D curve into another. Such transformations are of crucial importance to 2-D recognition, motion and tracking.

Many methods have been proposed to evaluate the parameters of the transformation of a 2-D curve into another. Such techniques can be classified into local and global: the latter are based on matching a global vector of features, and thus suffer from occlusion; the former use local features (such as curvature), which depend only upon portions of objects [2, 11].

Due to their local nature, points of significant curvature have received special attention in computing the parameters of the transformation in 2-D and 3-D recognition problems [7, 22, 5]. Extensive work has been devoted to the estimation of curvature [18, 22, 21, 19], in general, and to the detection of points of significant curvature, particularly corners [14, 3, 12, 15, 10, 20]. A comprehensive comparison of curvature estimation methods has been reported in [24]. More recently, the results of a series of experiments on three different estimators of point curvature in varying degrees of noise were published [9]; therein it is shown that the effectiveness of leading existing algorithms depends crucially upon the choice of the appropriate smoothing factor (*i.e.*, region of support).

Cohen *et al.*, proposed a method for determining transformations between two curves. This method is based on the minimisation of energy which tends to preserve the matching of points of significant curvature, while ensuring a smooth field of displacement vectors everywhere [6]. However, this technique is suited for deformable curves, and is very expensive since it requires the solution of a second order partial differential equation. Furthermore, the method also requires a first guess to start the iterative solution of the differential equation, and does not explicitly solve for the parameters of the transformation.

Ma and Chen's technique is based on a Generalised Hough transform [13], and can be summarised as follows:

For a given pair of boundaries  $M$  and its affine transform  $N$ , let  $(m, n) \in M \times N$  be a pair of corresponding points on the continuous curves  $M$  and  $N$ . Asserting that  $m = (x(t), y(t))^T$  corresponds to  $n = (u(t), v(t))^T$  gives:

$$\begin{bmatrix} x(t) \\ y(t) \end{bmatrix} = kR \begin{bmatrix} u(t) \\ v(t) \end{bmatrix} + \begin{bmatrix} x_0 \\ y_0 \end{bmatrix} \quad (1)$$

---

\*The author is now with the Faculty of Science and Engineering, Al-Akhawayn University in Ifrane, Hassan II Avenue, PO. BOX 104, 53 000 Ifrane e, Morocco.

where  $k$  is the expansion factor,  $X_0 = (x_0, y_0)^T$  is the translation vector and  $R$  is the rotation matrix:

$$R = \begin{bmatrix} \cos\theta & -\sin\theta \\ \sin\theta & \cos\theta \end{bmatrix}$$

The slope and curvature at a point  $m = (x(t), y(t))^T$  on a continuous curve parametrised by  $t$  are given by:

$$\text{tg}(\alpha) = \frac{y'}{x'} \quad (2)$$

$$\zeta = \frac{x'y'' - y'x''}{(x'^2 + y'^2)^{\frac{3}{2}}} \quad (3)$$

where  $x' = dx/dt$ ,  $x'' = d^2x/dt^2$ ,  $y' = dy/dt$  and  $y'' = d^2y/dt^2$ .

After some elementary mathematics, the slope angles  $\alpha_i$  and  $\beta_i$  on corresponding points  $m_i$  and  $n_i$  are related by:

$$\text{tg}(\alpha_i - \beta_i) = \text{tg}(\theta) \quad (4)$$

Additionally, the curvatures  $\zeta_i$  and  $\gamma_i$  on corresponding points  $m_i$  and  $n_i$  obey the equation:

$$\zeta_i = \frac{1}{k} \gamma_i \quad (5)$$

Ma and Chen's algorithm is as follows:

1. Form two two-dimensional accumulator arrays  $A(X_0)$  and  $B(k, \theta)$ ,
2. For every pair of points  $(m_i, n_i) \in M \times N$ , compute  $(k, \theta, x_0, y_0)$  using the above equations, and increment  $A(X_0)$  and  $B(k, \theta)$ .

Local maxima in  $A(X_0)$  and  $B(k, \theta)$  correspond to the parameters of the transformation.

There are a number of intrinsic problems with this approach:

- the complexity of the method is given by the size  $M \times N$ .
- due to the sensitivity of curvature to perturbations and noise, the obtained values for  $k$  (ratio of curvatures) lack precision;
- the approach does not cope well with curves containing points where curvature is undefined, such as perfect corners (see **Figure 1**). In implementing Ma and Chen's technique, we used Spline functions to approximate curves. Although curve  $C'$  in **Figure 1** is obtained by expanding curve  $C$ , no expansion factor was found (*i.e.*,  $k = 1$ ). This is due to the fact that curvatures are the same at both corners (see **Figure 2**);

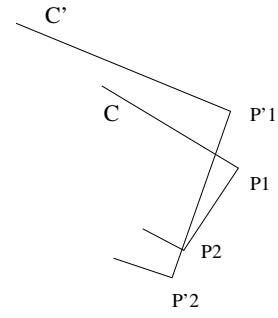


Figure 1. The curve  $C'$  was obtained by rotating and expanding the curve  $C$ .

- the problem with the above example goes beyond implementation. It actually reflects the locality of the technique. That is, the aperture problem [23]. Through a small aperture placed over the corner, as shown in **Figure 3**, it is impossible to say if an expansion is occurring or not. Of course, if there is another point of high curvature within the aperture, then the combination of local measurements at these points can yield the expansion rate.

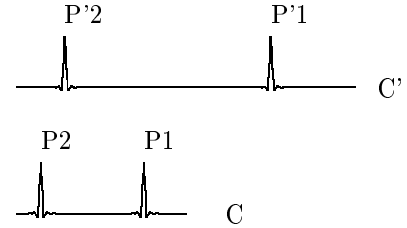


Figure 2. Curvature profiles for  $C$  and  $C'$  (**Figure 1**) computed from a Spline approximation. Corners  $P1$  (resp.  $P2$ ) and  $P'1$  (resp.  $P'2$ ) have the same curvature. Hence, the erroneous expansion of 1.

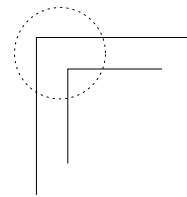


Figure 3. The aperture problem, looking at the expanding boundary through a small aperture, it is impossible to determine the expansion factor at corners.

## 2 Establishing Motion Parameters

In perceiving the motion of **Figure 1**, it appears that the human visual system uses the distances between corners of each curve to work out the expansion, and uses the orientation of the lines joining these corners to derive the rotation<sup>1</sup>. Looking at the locations of all points of significant curvature within the same boundary is a global approach which overcomes the aperture problem.

Based on this remark, the parameters of the transformation can be defined as follows:

$$k = \frac{\|P'1\vec{P}'2\|}{\|P1\vec{P}2\|} \quad (6)$$

$$\theta = \text{acos} \left[ \frac{P'1\vec{P}'2 \cdot P1\vec{P}2}{\|P'1\vec{P}'2\| \cdot \|P1\vec{P}2\|} \right] \quad (7)$$

$$X_0 = P'1 - kR.P1 \quad (8)$$

where  $k$  is the expansion factor,  $\theta$  the angle of rotation, and  $X_0$  the translation vector.

What seems important then is not so much the value of the curvature at the corners, but the locations of these corners – points of maximum curvature, in general. These points are sometimes called critical (or salient) points [1].

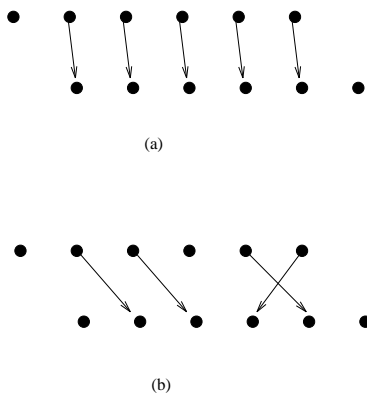


Figure 4. *Bullets designate significant curvature points. Arrows indicate pairings. (a) allowed configuration. (b) disallowed configuration because of the crossing.*

<sup>1</sup>We have no proof for these claims. This matter may be a fruitful topic of research in psychology, in which measurements of perception of expansion and rotation using curvature on the one hand, and positions of high curvature points, on the other hand, are compared.

## 3 Moving the Goal Post

Finding the parameters of motion is posed as a matching problem in this work, that is, establishing correspondence between peaks (points of significant curvature). The actual evaluation of the parameters is obtained from the resulting pairings.

This matching must be a one-to-one, and without crossings (see **Figure 4**). The first constraint (*i.e.*, one-to-one) stems from the physical nature of points of high curvature, *i.e.*, a point of high curvature in the scene always projects into a unique point in the image plane. The second constraint (*i.e.*, prohibition of crossings) is dictated by the natural ordering on boundary points. The ordering not only allows straightforward processing and measurements, but must also be satisfied by all plausible solutions.

Additionally, if such matching exists for a solid boundary undergoing a transformation, “proportionality” must be conserved between pairs of corresponding peaks. Let  $P_1, P_2, \dots, P_n$  be the ordered peak points on  $C$ , and let  $P'_1, P'_2, \dots, P'_n$  be their corresponding peak points on  $C'$ . Let

$$k_{i,j} = \frac{\|P'_i P'_j\|}{\|P_i P_j\|} \quad \forall i, j \in \{1..n\}, \quad i \neq j \quad (9)$$

$k_{i,j}$  represents the expansion that the curve  $C$  undergoes to become  $C'$ , estimated here from  $P_i, P'_i, P_j$  and  $P'_j$ . Because of the rigidity assumption, the expansion factor is the same for all pairs of corresponding peaks (see **Figure 5**).

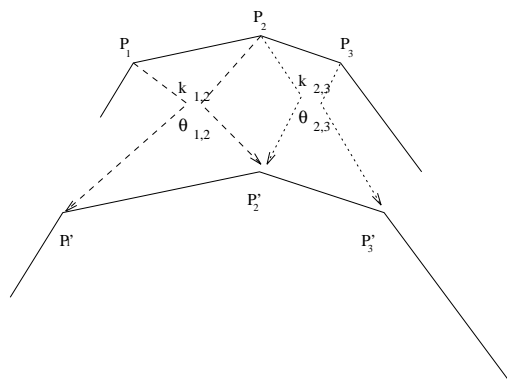


Figure 5. *Expansion factors are equal i.e.,  $k_{1,2} = k_{2,3}$ . Similarly the angles of rotation are equal i.e.,  $\theta_{1,2} = \theta_{2,3}$ .*

Thus, the proportionality constraint may be written as follows:

$$\forall i, j \in \{1..n\}, i \neq j, \forall h, l \in \{1..n\}, h \neq l,$$

$$[k_{i,j} = k_{h,l}] \quad (10)$$

In practice, such a constraint is very strong, and has to be relaxed to allow for small differences between the different  $k_{i,j}$ . Moreover, it is not necessary to consider all pairs of points  $P_i, P'_i, P_j, P'_j, P_h, P'_h, P_l$  and  $P'_l$ . It can be shown that the subset of successive points  $P_i, P'_i, P_{i+1}, P'_{i+1}, P_{i+2}$  and  $P'_{i+2}$  gives a sufficient constraint. In the light of the above remark, the proportionality constraint is then expressed as follows:

$$\forall i \in \{1..n-2\}, [|k_{i,i+1} - k_{i+1,i+2}| \leq \epsilon_1] \quad (11)$$

where  $\epsilon_1$  is a small number representing the maximum difference allowed. Typically  $\epsilon_1 = 0.05$ .

This constraint is computationally less expensive than (10), since only a subset of all the possible combinations of pairs of peaks, satisfying the ordering constraint, is considered.

Similarly, a second constraint can be derived for the angle of rotation  $\theta$ . Let  $\theta_{i,j}$  represent the angle of rotation that curve  $C$  undergoes to become  $C'$ , estimated from  $P_i, P'_i, P_j$  and  $P'_j$ . Because of the rigidity assumption, this angle is the same for all pairs of corresponding peaks. Thus, the second proportionality constraint can be written as follows:

$$\forall i \in \{1..n-2\}, [|\theta_{i,i+1} - \theta_{i+1,i+2}| \leq \epsilon_2] \quad (12)$$

where  $\epsilon_2$  is a small number representing the maximum difference allowed in the angle of rotation. Typically  $\epsilon_2 = 5^\circ$ .

The two constraints above (11) and (12) not only reduce the complexity of the process by a great deal, but also categorically discard wrong peaks (*i.e.* those which constitute noise and digitisation), since such peaks would obviously not satisfy the constraints.

Further, such correspondence should be “loose” at both ends of each boundary, that is, it should allow genuine peaks at boundary ends not to be matched. Such peaks may be present due to occlusion (see **Figure 6**).

Consequently, the desired matching is the longest one (*i.e.*, the one with the maximum number of corresponding peaks) satisfying all the above constraints. Theoretically, such a matching exists and is unique.

The expansion factor  $k$  is calculated from the estimated expansions  $k_{i,i+1}$  of the final matching as follows:

$$k = \frac{1}{n-1} \sum_1^{n-1} k_{i,i+1} \quad (13)$$

similarly the final angle of rotation is obtained by averaging the angles  $\theta_{i,i+1}$  of the final matching:

$$\theta = \frac{1}{n-1} \sum_1^{n-1} \theta_{i,i+1} \quad (14)$$

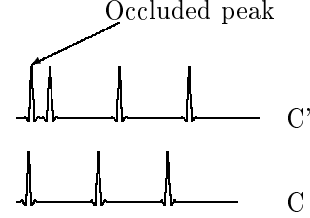


Figure 6. Profiles of curvature. Peaks at boundary ends may be occluded.

## 4 Constrained Peak Matching

Curvature profiles are computed from cubic Spline approximations of each curve. However, it is not necessary to compute the curvature. Only the locations of points of maximum curvature are of interest here. Peak locations for each curve are then stored in arrays  $R$  and  $R'$  for processing.

Note that at least two significant peaks (*i.e.*, two points of high curvature) must be present in  $C$  and in  $C'$ . Curves which do not satisfy this condition are called “simple” curves, and are ignored.

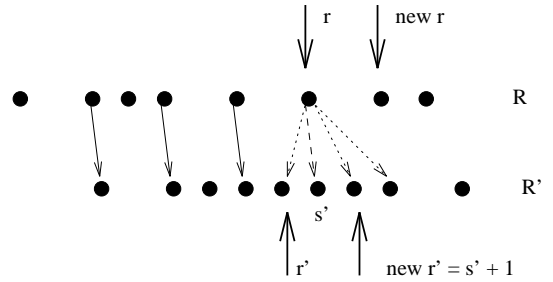


Figure 7. Establishing correspondence between peaks. Peak  $r$  is currently under examination. Among the  $M$  possible pairings (marked with dotted arrows),  $s'$  (marked with a dashed arrow) is the pairing consistent with the previously established pairs (marked with solid arrows). The search continues with the peak marked new  $r$  under focus, and with  $r' = s' + 1$ .

To find the longest match satisfying the above constraints, an exhaustive search is employed. Progressing from left to right, peaks from  $R$  and  $R'$  are tested in the following manner: let  $L = \{(p, p')\}$  be the list of peaks matched at a given stage; by construction, pairs in  $L$  satisfy the above conditions. Initially  $L = \emptyset$ . Let  $r$  and  $r'$  be the indices of the current peaks of  $R$  and  $R'$  under focus (see **Figure 7**). For all peaks between  $r'$  and  $r' + M$ , select  $s'$  such that the new pair  $(r, s')$  is consistent with all existing pairs in  $L$ . If such a peak exists, add  $(r, s')$  to  $L$ . If  $\sharp L > \sharp B$ , (where  $B$  is the previously best recorded match, and  $\sharp B$  its size), record  $L$  as the new best match, and continue with  $r = r + 1$  and  $r' = s' + 1$ . If, however, no peak between  $r'$  and  $r' + M$  can be consistently paired with  $r$ , continue with  $r = r + 1$ .

The number of potential peaks from  $R'$  under scrutiny each time is a global parameter of the process, typically  $M = 3$ .

The algorithm is as follows:

```

Search(R,N,r,R',N',r',L,l)

ARRAYS of PEAKS R,R'
LENGTHS N,N'
INDICES r,r'
LIST of PAIRS L
LENGTH l

BEGIN
  IF (r ≥ N OR r' ≥ N') THEN
    RETURN;

  FOR i=r' TO r'+M DO
    IF Consistent(R[r],R'[i],L,l) THEN
      L ← L ∪ {(r,i)} ;
      Search(R,N,r+1,R',N',i+1, L, l+1);
      IF Improvement(L,B) THEN
        L = B;
      END
    END
  END
END
END

```

Algorithm 4.1. *Algorithm for Constrained Peak Matching.*

$Improvement(L,B)$  determines whether there is an improvement in the pairings of  $L$  with respect to the best recorded pairings at the time of the call. Clearly, if  $L$  contains more pairings than  $B$ , an improvement has occurred. If, however, the lists  $B$  and  $L$  have the same number of pairs,  $L$  is said to be better than  $B$  if the pairings in  $L$  give a smaller rotation angle than

the pairings in  $B$ . This only happens when there is an intrinsic ambiguity in the affine transform.

The function  $Consistent(P,P',L,l)$  returns 1 if the pair  $(P,P')$  is consistent with the list of pairings  $L$  (of length  $l$ ) at the time of the call. The pair  $(P,P')$  is said to be consistent with  $L$  if the two ‘proportionality’ constraints on the expansion factor and the angle of rotation are satisfied for the list  $L \cup \{(P,P')\}$ .

The search is initiated with the following instructions:

```

B = ∅;
FOR i=0 TO M DO
  Search(R,N,i,R',N',0,∅,0);
END

```

## 5 The Complexity of the Algorithm

Let  $P(n)$  be the complexity of the procedure  $Search$ , where  $n$  is the number of peaks in the boundary  $C$ , we have:

$$P(n) = \alpha + pM(P(n-1) + \beta) + (1-p)$$

where  $\alpha$  is a constant accounting for the first **IF** statement,  $p$  the probability of success of the condition **IF Consistent**, and  $\beta$  a constant accounting for the **IF Improvement** statement. As stated earlier,  $M$  is the number of potential pairings tested for each peak.

Among the  $M$  potential pairings, only one<sup>2</sup> satisfies the consistency test. Hence  $p = 1/M$ . The expression of  $P(n)$  can be rewritten as:

$$P(n) = \alpha + P(n-1) + \beta + 1 - \frac{1}{M}$$

If we put the constant  $\gamma = \alpha + \beta + 1 - \frac{1}{M}$  we have:

$$P(n) = \gamma + P(n-1)$$

By recursively substituting  $P(n-1)$  in  $P(n)$ , we obtain:

$$P(n) = n\gamma$$

Since the procedure  $Search$  is called  $M$  times, it follows that the complexity of the approach is  $O(n) = Mn$ .

<sup>2</sup>If more than one does, they must be at the same position, and hence are the same.

## 6 Generalisation

The Constrained Peak Matching technique can be generalised to find the parameters of the full affine transformation. Such transformation includes rotation, translation, expansion and skewing.

$$\begin{aligned} u &= a^{(0)} + a^{(1)}x + a^{(2)}y \\ v &= a^{(3)} + a^{(4)}x + a^{(5)}y \end{aligned} \quad (15)$$

where  $a^{(i)}$ ,  $i \in \{0..5\}$ , are six unknown coefficients,  $(u, v)^T$  and  $(x, y)^T$  are pairs of corresponding points on the two curves. In order to find the six unknown coefficients  $a^{(i)}$ ,  $i \in \{0..5\}$ , three pairs of peaks are to be considered.

If  $C$  is a boundary undergoing such transformation, the parameters  $a^{(i)}$ ,  $i \in \{0..5\}$ , must be the same for any three pairs of corresponding peaks. Let  $P_1, P_2, \dots, P_n$  be the ordered peak points on  $C$ , and let  $P'_1, P'_2, \dots, P'_n$  be their corresponding peak points on  $C'$ . Let  $a_{i,j,k}^{(l)}$  be the coefficients estimated from peaks  $P_i, P'_i, P_j, P'_j, P_k$  and  $P'_k$ , by solving the system of six linear equations obtained from these points. The constraint on  $a_{i,j,k}^{(l)}$  can be expressed as follows:

$$\begin{aligned} \forall l \in \{0..5\}, \quad \forall i \in \{1..n-3\}, \\ \left[ |a_{i,i+1,i+2}^{(l)} - a_{i+1,i+2,i+3}^{(l)}| \leq \epsilon_l \right] \end{aligned} \quad (16)$$

where  $\epsilon_l$  is a small number representing the maximum differences allowed for  $a^{(l)}$ .

The parameters are given by the correct matching (*i.e.*, the longest one with the maximum number of corresponding peaks) satisfying all the constraints of (16). Note that not all the constraints are needed: depending on the context, some constraints can be dropped.

The algorithm is essentially the same as **Algorithm 4.1**. As stated earlier such matching, in theory, exists and is unique. The final value of the coefficient  $a^{(l)}$  is defined to be:

$$a^{(l)} = \frac{1}{n-2} \sum_1^{n-2} a_{i,i+1,i+2}^{(l)} \quad \forall l \in \{0..5\} \quad (17)$$

However, unlike the restricted model presented earlier, the coefficients  $a^{(i)}$ ,  $i \in \{0..5\}$ , have no direct intuitive interpretations. This renders the choice of the differences allowed  $\epsilon_i$ ,  $i \in \{0..5\}$ , more empirical. Additionally, solving the linear system may turn out to be costly. In fact, in the restricted model, a linear system of four equations and four unknowns ( $k, \theta, t_x, t_y$ ) was implicitly solved in equations (6)–(8).

The Constrained Peak Matching technique can be applied to a variety of problems involving boundaries/contours. For instance, it can be used to find the axes of skewed symmetry [4]. The following constraints on the parameters  $a^{(i)}$ ,  $i \in \{0..1\}$  of the axis  $y = a^{(0)}x + a^{(1)}$  can be used:

$$\begin{aligned} \forall l \in \{0..1\}, \quad \forall i \in \{1..n-2\}, \\ \left[ |a_{i,i+1}^{(l)} - a_{i+1,i+2}^{(l)}| \leq \epsilon_l \right] \end{aligned} \quad (18)$$

where  $a_{j,k}^{(l)}$ ,  $l \in \{0..1\}$  are obtained from points  $P_{j/2}$  and  $P_{k/2}$  (see **Figure 8**) in the following manner:

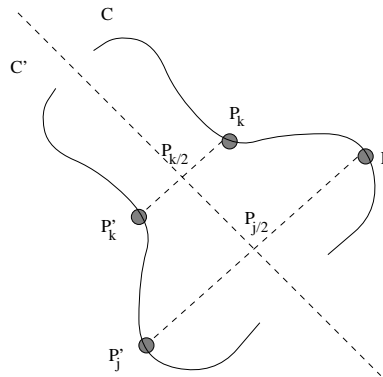


Figure 8. Parameters  $a_{j,k}^{(l)}$ ,  $l \in \{0..1\}$  are computed from points  $P_{j/2}$  and  $P_{k/2}$  which are derived from corresponding Peaks  $(P_j, P'_j)$  and  $(P_k, P'_k)$ .

Let  $P_{k/2} = (x_{k/2}, y_{k/2})^T$  and  $P_{j/2} = (x_{j/2}, y_{j/2})^T$  be the respective midpoints of segments  $[P_j, P'_j]$  and  $[P_k, P'_k]$ , we have:

$$a^{(0)} = \frac{y_{k/2} - y_{j/2}}{x_{k/2} - x_{j/2}} \quad (19)$$

$$a^{(1)} = y_{k/2} - a^{(0)}x_{k/2} \quad (20)$$

## 7 Evaluating the Method

The number of pairs obtained is a good indication of the correctness of computed transformation; if this number is not large enough, it can be easily decided that the parameters of the affine transform could not be computed using this technique. This is the case for straight lines. In 2-D recognition, if a data curve and a model curve have enough points of significant curvature, but the number of pairings between them is low, a decision can be taken to reject the curve as part

of a model object. In motion context, a low number of pairings implies that the model used for computing motion (*i.e.*, the Affine transform model) does not fit the physical changes in the scene. In fact, the ratio

$$r = \frac{p}{n} \quad (21)$$

where  $p$  is the number of paired peaks, and  $n$  is the smallest of number of peaks of the two curves, is a self-verifying indicator of the goodness of the model. The computed affine transform parameters are taken to be reliable if  $r \geq 0.5$ , which implies that 50% of the points of significant curvature are correctly matched in accordance with the constraints.

## 8 Results

In this section, we present results of the computation of the parameters of the affine transform. Comparisons are drawn with Ma and Chen’s technique, which was actually implemented for this purpose.

Boundary	Method	$k$	$\theta$	$(t_x, t_y)$
(a)	HT	1.0	$90^\circ$	(52,2)
	AC	2.0	$0^\circ$	(10,10)
	CPM	2.0	$0^\circ$	(10,10)
(b)	HT	0.99	$0^\circ$	(6,15)
	AC	1.0	$8^\circ$	(5,10)
	CPM	1.009	$8^\circ$	(5,11)
(c)	HT	1.0	$-9^\circ$	(-2,1)
	AC	2.3	$10^\circ$	(-5,10)
	CPM	2.27	$10^\circ$	(-4,10)
(d)	HT	0.98	$60^\circ$	(19,12)
	AC	2.0	$4^\circ$	(-5,10)
	CPM	1.98	$4^\circ$	(-5,10)

Table 1. *The parameters computed by the Hough Transform method (HT) and by our method: Constrained Peak Matching (CPM). (AC) are the actual parameters. See Figure 9 for curves (a), (b), (c) and (d).*

Judging from the results displayed in [6], our technique performs at least as well as Cohen *et al.*’s for the particular case of boundaries undergoing *similarity* transformation (uniform deformation). It is also more conservative, for their technique is iterative and is based on a first guess.

Figure 9 (c) and (d) are designed to show that our technique accounts properly for disruptions (indicated by arrows) appearing at end points due to occlu-

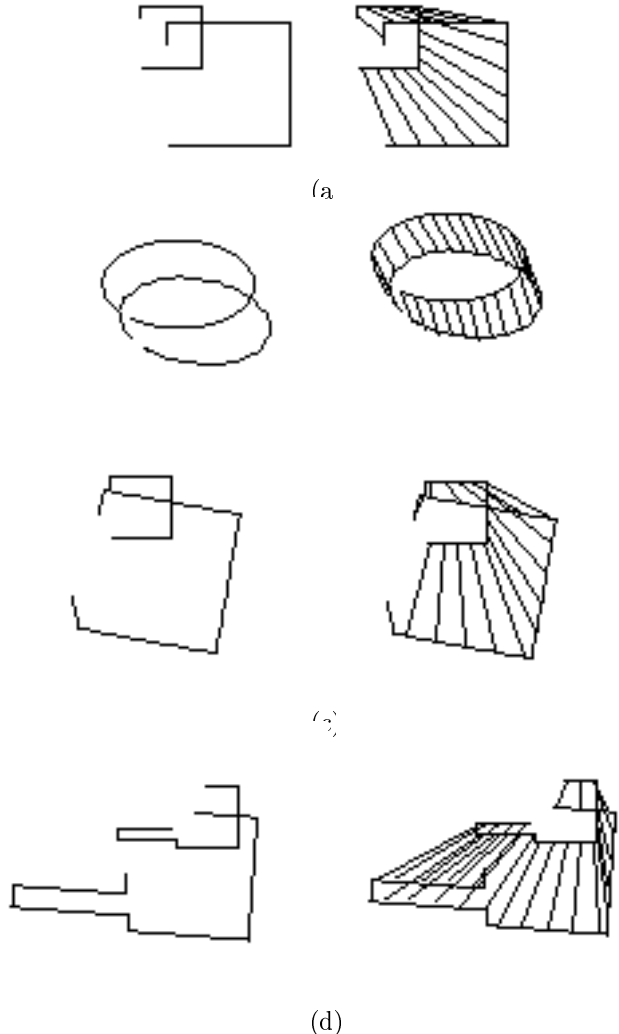


Figure 9. (a), (b), (c) and (d) are a set of artificial boundaries undergoing controlled transformations. The parameters computed for these transformations are displayed in Table 1, and sketched here by point-to-point mapping along the curves. Experiments (c) and (d) in particular, show the ability of our technique to deal with occlusion disruptions. These disruptions are indicated by arrows.

sion. The parameters found are the correct parameters which would transform one boundary to the other regardless of their differences at end points. Compare these results with those obtained with [11]’s method (see **Table 1**).

The following set of real experiments was performed as part of a correspondence-based object separation module [8]. Boundaries are first extracted from sequences of images [17], and their correspondence is established [16]. Due to the physical setting (conveyor belt) or to the nature of small movements, boundary motion is assumed to follow the affine transform model, which can be cross-checked *a posteriori*.

**Figure 11** shows the velocities obtained for the two successive frames of **Figure 10**. Note that the motion of the longest boundary has not been affected by the over-segmentation which resulted in joining two different boundaries. The number of high curvature points pairings on the top part of the boundary, satisfying the correct expansion  $k = 1.0$ , is large enough to override any perturbation arising from the lower part.

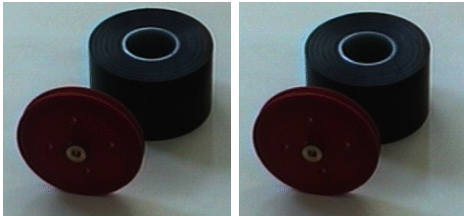


Figure 10. A real motion sequence in which the object at the back undergoes a translational motion to the left. This motion is assumed to follow the affine transform model.

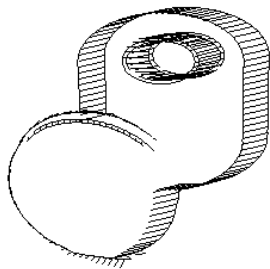


Figure 11. Mapping obtained for the two-frame sequence of **Figure 10**.

**Figure 13** shows the velocities obtained for the two successive frames of **Figure 12**.

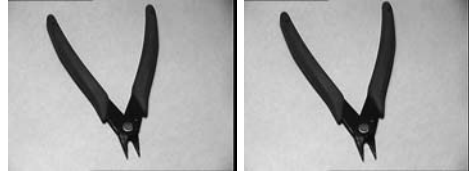


Figure 12. The image on the right was obtained by moving the camera forward. This movement follows the affine transform model.



Figure 13. Mapping obtained for the two-frame sequence of **Figure 12**, in which the wire snips undergo a small expansion, because of the forward motion of the camera.

**Figure 16** shows the velocities obtained by our approach and the Hough Transform approach for the two successive frames of **Figure 14**.

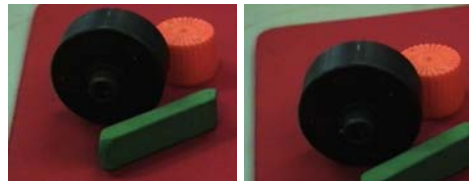


Figure 14. A simulated conveyor belt sequence: As the mouse pad is manually moved, the different objects undergoing a 3-D translation towards the camera. This motion is assumed to follow the Affine transform model.

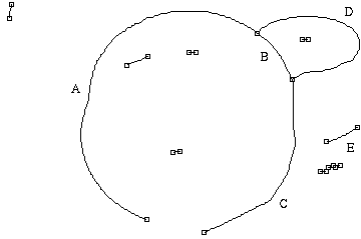


Figure 15. Boundaries extracted from the left image of the sequence of **Figure 14**.

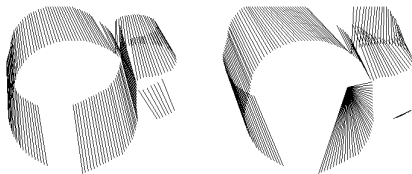


Figure 16. Left: the motions obtained by our technique. Right: the motions obtained with the Hough Transform approach for the sequence of frames in **Figure 14**.

Boundary	Method	$k$	$\theta$	$(t_x, t_y)$
Bdy A	HT	0.79	$0^\circ$	$(-73, -77)$
	CPM	0.80	$0^\circ$	$(-39, -63)$
Bdy B	HT	0.84	$-1^\circ$	$(-24, -48)$
	CPM	0.83	$0^\circ$	$(-26, 54)$
Bdy C	HT	0.01	$180^\circ$	$(-41, 11)$
	CPM	0.87	$0^\circ$	$(-27, -95)$
Bdy D	HT	0.98	$41^\circ$	$(5, -105)$
	CPM	0.66	$0^\circ$	$(1, -55)$
Bdy E	HT	0.0	$0^\circ$	$(0, 0)$
	CPM	1.33	$0^\circ$	$(-21, -53)$

Table 2. The parameters computed by the Hough Transform method (HT) and by our method: Constrained Peak Matching (CPM). See **Figure 15** for labels A, B, C, D and E.

In this sequence, the objects undergo a translation towards the camera, as a result of the forward motion of the mouse pad (to simulate a conveyor

belt). **Table 2** gives the values of the parameters obtained for the boundaries of the reverse sequence by the two methods. It can be seen clearly that the Hough Transform method *i.e.*, Ma and Chen’s, fails to find plausible parameters for boundary C. This is because of the occlusion effect, which our technique was designed to overcome. Also, the Hough Transform technique fails to find the correct parameters for boundary D. This, however, is due to the sub-optimality in curvature values computed by a crude method. Our technique, on the other hand, delivers correct parameters because curvature values are not used, but rather we use the locations of high curvature points. As expected, boundaries A, B and C all have similar expansion factors (0.80, 0.83 and 0.87). Boundary D on the other hand has a different expansion factor 0.66 which actually underlies the difference in depth with boundaries A, B and C. The parameters found for boundary E, however, are erroneous. This is because there is not a sufficient number of high curvature points to capture the motion. Note that Ma and Chen’s technique failed too.

These various experiments demonstrate the robustness of our approach to determine the parameters of the affine transform. This robustness stems from:

- the formulation of the parameters of motion, namely, the expansion and the angle of rotation in terms of high curvature points pairings rather than the curvature itself;
- the algorithm developed to establish the matching between points of significant curvature, which integrates the expansion factor and the angle of rotation to constrain the search space.

## Conclusion

The computation of the parameters of the  $2-D$  affine transform is posed as a correspondence between points of significant curvature. The parameters are then computed from the resulting pairings of ‘peaks’ of curvature. This formulation is novel, global (within the domain of the curve under focus), robust, and is able to overcome the differences due to occlusion at boundary endings. It also offers a natural means of measuring the plausibility of the model (via number of matches of high curvature points over the number of high curvature points of both boundaries). In addition, the integration of the parameters to the matching, and the use of the natural ordering of high curvature points along boundaries, render

this technique very conservative  $O(Mn)$ , where  $M$  is a small constant, unlike in existing techniques, which are either iterative or are based on the Hough transform. Finally, we showed that this technique can be generalised to a variety of problems, particularly to determining the axes of symmetry.

## Acknowledgements

This work was partially supported by an ORS award. The code for computing Spline approximation was provided by Mr. Saloustros.

## References

- [1] H. Asada and J. M. Brady. The curvature primal sketch. *IEEE Transactions on Pattern Analysis and Machine Intelligence*, 8(1):2–14, 1986.
- [2] N. Ayache and O. D. Faugeras. Hyper: a new approach for the recognition and positioning of two dimensional objects. *IEEE Transactions on Pattern Analysis and Machine Intelligence*, PAMI-8(1), 1986.
- [3] M. Brady. Seeds of perception. In *Proceedings of the Third Alvey Vision Conference, (Cambridge University, 15–17 September)*, pages 259–266. The University of Sheffield Printing Unit, 1987.
- [4] Tat-Jen Cham and Roberto Cipolla. Skewed symmetry detection through local skewed symmetries. In *Proceedings of the 5th British Machine Vision Conference*, volume 2, pages 549–558, York, September 1994.
- [5] C. H. Chien and J. K. Aggarwal. Model construction and shape recognition from occluding contours. *IEEE Transactions on Pattern Analysis and Machine Intelligence*, 1(4):372–389, 1989.
- [6] Isaac Cohen, Nicholas Ayache, and Patrick Sulger. Tracking points on deformable objects using curvature information. In *Second European Conference on Computer Vision*, pages 458–466, 1992.
- [7] L. S. Davis. Shape matching using relaxation algorithms. *IEEE Transactions on Pattern Analysis and Machine Intelligence*, 1:60–72, 1979.
- [8] Tajje eddine Rachidi. *Separating Solid Objects using the Correspondence of Boundaries*. PhD thesis, Department of Computer Science, University of Essex, Colchester CO4 3SQ, U.K., December 1994.
- [9] D. P. Fairney and P. T. Fairney. On the accuracy of point curvature estimators in a discrete environment. *Image and Vision Computing*, 12(5):259–265, 1994.
- [10] Chris Harris and Mike Stephens. A combined corner and edge detector. In *Proceedings of the Fourth Alvey Vision Conference (Manchester University, 31st August–2nd September)*, pages 147–152. The University of Sheffield Printing Unit, 1988.
- [11] Song De Ma and Xing Chen. Hough transform using slope and curvature as local properties to detect arbitrary 2-d shapes. *IEEE International Conference on Pattern Recognition*, 1:511–513, 1988.
- [12] Gerard Medioni and Yoshio Yasumoto. Corner detection and curve representation using cubic b-splines. *Computer Vision, Graphics and Image Processing*, 39:267–278, 1987.
- [13] Philip M. Merlin and David J. Farber. A parallel mechanism for detecting curves in pictures. In *IEEE Transactions on Computers*, pages 96–98, January 1975.
- [14] J. A. Noble. Finding corners. In *Proceedings of the Third Alvey Vision Conference, (Cambridge University, 15–17 September)*, pages 267–274. The University of Sheffield Printing Unit, 1987.
- [15] J. Alison Noble. Finding corners. *Image and Vision Computing*, 6(2):121–128, May 1988.
- [16] T. Rachidi and L. Spacek. Boundary-based correspondence computation using the topology constraint. In *Proceedings of the 5th British Machine Vision Conference*, volume 1, pages 55–64, York, September 1994.
- [17] T. Rachidi and L. Spacek. Constructing coherent boundaries. In *Proceedings of the 5th British Machine Vision Conference*, volume 1, pages 296–304, York, September 1994.
- [18] A Rosenfeld and E. Johnston. Angle detection on digital curves. *IEEE Transactions on Computers*, 22:875–878, 1973.
- [19] Zhimin Shao and Josef Kittler. Estimating angles and curvature features in grey scale images. In *British Machine Vision Conference*, volume one, pages 115–124, Sep 1994.
- [20] Ajit Singh and Michael Shneier. Grey level corner detection: A generalisation and a robust real time implementation. *Computer Vision, Graphics and Image Processing*, 51:54–69, 1990.
- [21] Libor Spacek. *The Detection of Contours and their Visual Motion*. PhD thesis, University of Essex, UK, 1986.
- [22] T. P. Wallace, O. R. Mitchell, and K. Fukunaga. Three dimensional shape analysis using local shape descriptors. *IEEE Transactions on Pattern Analysis and Machine Intelligence*, 3(3):310–323, 1984.
- [23] H. Wallach, editor. *On Perception*, chapter On Perceived Identity: 1. The Direction of Motion of Straight Lines. Quadrangle, New York, 1976.
- [24] M. Worring and A. W. M. Smeulders. The accuracy and precision of curvature estimation methods. In *IAPR*, volume 3, pages 139–, 1992.